Interaction between heterogeneously charged surfaces: Surface patches and charge modulation

Dan Ben-Yaakov and David Andelman[*]

Raymond & Beverly Sackler School of Physics and Astronomy, Tel Aviv University, Ramat Aviv, Tel Aviv 69978, Israel

Haim Diamant

Raymond & Beverly Sackler School of Chemistry, Tel Aviv University, Ramat Aviv, Tel Aviv 69978, Israel

When solid surfaces are immersed in aqueous solutions, some of their charges can dissociate and leave behind charged patches on the surface. Although the charges are distributed heterogeneously on the surface, most of the theoretical models treat them as homogeneous. For overall non-neutral surfaces, the assumption of surface charge homogeneity is rather reasonable since the leading terms of two such interacting surfaces depend on the nonzero average charge. However, for overall neutral surfaces the nature of the surface charge distribution is crucial in determining the intersurface interaction. In the present work we study the interaction between two charged surfaces across an aqueous solution for several charge distributions. The analysis is preformed within the framework of the linearized Poisson-Boltzmann theory. For periodic charge distributions the interaction is found to be repulsive at small separations, unless the two surface distributions are completely out-of-phase with respect to each other. For quenched random charge distributions we find that due to the presence of the ionic solution in between the surfaces, the intersurface repulsion dominates over the attraction in the linear regime of the Poisson-Boltzmann theory. The effect of quenched charge heterogeneity is found to be particularly substantial in the case of large charged domains.

PACS number(s): 68.08.−p, 82.70.Uv, 41.20.Cv, 87.16.dr

I. INTRODUCTION

Long-range interactions between charged surfaces substantially influence the structural properties of soft materials, such as lipid membranes and colloidal suspensions [1–3]. The nature of the long-range interaction between two charged surfaces immersed in an ionic solution is mainly determined by electrostatic interactions, mediated by the ionic solutes and polar solvent. When modeling the electrostatic interaction, surfaces are usually assumed to be homogeneously charged [1,4–6]. However, most charged surfaces in soft matter are heterogeneous over a certain length scale. A schematic drawing of two such heterogeneously charged surfaces is presented in Fig. 1. While the interaction between two homogeneous surfaces depends on the average surface charge and the intersurface separation, the interaction between two heterogeneous surfaces depends on the intra- and intersurface charge correlations as well.

Several experimental studies [7–17] measured intersurface forces for different configurations of surface charge heterogeneities. For example, it was demonstrated [7–15] that coating a negatively charged mica surface with a cationic surfactant monolayer may lead to the formation of positively charged bilayer patches, which neutralize the negative patches of the bare mica. A long-range attractive force was measured [7–15] between two such coated mica surfaces. In another setup, it was found that adsorption of positive polyelectrolytes on negatively charged spherical beads can lead to charge inversion of the beads [16,17]. The adsorbed polyelectrolyte forms positively charged domains, while patches of bare regions on the beads remain negatively charged. It has been shown [17] that by controlling the amount of adsorbed polyelectrolyte, overall neutral particles with a patchy heterogeneous charge distribution can be prepared. In this special case of neutral beads, the interparticle interaction is attractive, while for smaller or larger amount of adsorbed polyelectrolyte (where the average bead charge is, respectively, negative or positive) the interaction is repulsive.

The interaction between two *periodically ordered* charged surfaces has been studied theoretically in several works [18–26] within the framework of the linearized Poisson-Boltzmann (PB) equation. For non-neutral surfaces, the leading interaction term depends on the average charge. For neutral surfaces, where the average charge is zero, the interaction depends strongly on the relative phase between the two charge distributions and can vary from being repulsive to attractive. For two surfaces with identical average charge and small amplitude charge modulation it was shown, in the nonlinear regime, that the repulsive interaction is weaker than the repulsion between two uniformly charged surfaces with the same average charge [27–32]. However, for nonzero average charge, the charge modulation leads only to a small correction, as compared to the leading interaction term determined by the average charge.

In a more general case of experimental relevance the surface charges are distributed *randomly* (and not periodically). We further make the important distinction between quenched and annealed cases of surface charge disorder. In the *annealed* case, the surface charges are in thermodynamic equilibrium with other system variables, such as intersurface separation, temperature, and concentration of other species. The attraction can then be caused by self-adjusting of surface charged domains, where positively charged patches on one surface position themselves against negatively charged patches on the second surface and vice versa [33–36]. For this case to
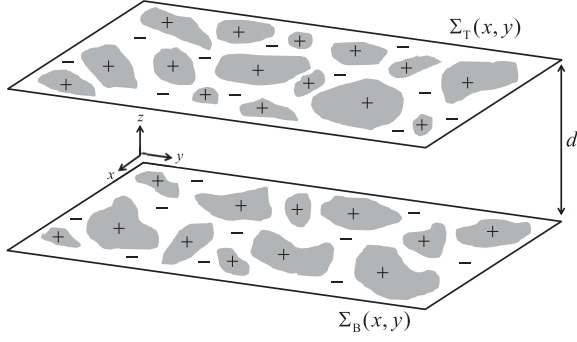
———————
[*]andelman@post.tau.ac.il

FIG. 1. Schematic drawing of two planar heterogeneously charged surfaces immersed in ionic solution. The gray regions are positively charged, and the white ones are negatively charged. The charge distributions of the bottom and top surfaces are given by $\Sigma_B(x,y)$ and $\Sigma_T(x,y)$, respectively. The intersurface separation is d.

hold, the typical time scale of patch rearrangement must be substantially shorter than the measurement time scale, such that the self-adjustment (annealing) of charged domains on the surfaces has enough time to be completed.

In the *quenched* case, the surface charges are frozen and independent of other system variables. For a quenched distribution of surface charges with no inter- and intrasurface correlations, it was reported that such heterogeneities have no effect on the two-surface interaction at the mean-field level [37,38], and the interaction depends solely on the average surface charge.

Another interesting case of quenched disorder, to be considered in detail in the present work is the case where finite-size charged domains (patches) are randomly distributed on each surface. In some of the experiments such random charged domains stem from the specific surface preparation [7–15].

The outline of our paper is as follows. The model is formulated in Sec. II. In Sec. III the interaction between surfaces with periodic charge modulations is revisited and a crossover from attraction to repulsion is discussed. Quenched random charge distributions are treated in Sec. IV for several cases within the linear regime of the PB equation. In particular, the limit of small domains having a size in the molecular range is compared with the limit of large domains. In Sec. V we discuss the implications of our results, and concluding remarks are presented in Sec. VI. Finally, in the limit of infinitely large charged domains, we compare in the Appendix the predictions of the linear regime to those of the nonlinear one considered in Ref. [15], where an attractive intersurface interaction was predicted in the limit of infinitely large charged domains. An interesting crossover is found from intersurface attraction of strongly charged surfaces to repulsion for weakly charged surfaces, emphasizing even further the role of the domain lateral size.

II. THE LINEAR POISSON-BOLTZMANN MODEL

We consider an aqueous solution as depicted in Fig. 1, which is confined between two semi-infinite and planar charged surfaces, located at $z = \pm d/2$, where the $\hat{z}$ axis is perpendicular to the surfaces. The surface-charge density

distribution (charge per unit area) is given by $\Sigma_B(x,y)$ for the bottom surface at $z = -d/2$, and $\Sigma_T(x,y)$ for the top one at $z = d/2$. As we are interested in the effect of *quenched* charge heterogeneity, we model the lateral surface charge distributions Σ_B and Σ_T as fixed charge boundary conditions. Namely, they are frozen and independent of other system variables.

The aqueous solution contains a 1:1 monovalent salt ions. The solvent (water) is modeled as a homogeneous dielectric background with dielectric constant $\varepsilon = 80$. The solution is coupled to a reservoir of ionic density n_b. The electrostatic potential, ψ, and the ionic densities, $n_\pm = n_b e^{\mp e\psi/k_B T}$, are calculated via the Poisson-Boltzmann (PB) equation:

$$\nabla^2 \psi = \frac{8\pi e n_b}{\varepsilon} \sinh(e\psi/k_B T), \tag{1}$$

where e is the electron charge, $k_B T$ is the thermal energy, and k_B is the Boltzmann constant. By rescaling the potential $\psi \rightarrow \phi \equiv e\psi/k_B T$ the PB equation is rewritten for ϕ, the dimensionless electrostatic potential, as

$$\nabla^2 \phi = \kappa_D^2 \sinh\phi, \tag{2}$$

where $\kappa_D = \lambda_D^{-1} = \sqrt{8\pi l_B n_b}$ is the inverse Debye screening length and $l_B = e^2/(\varepsilon k_B T)$ is the Bjerrum length. The boundary conditions at $z = \pm d/2$ are given by

$$\left.\frac{\partial \phi}{\partial z}\right|_{-d/2} = -\sigma(x,y), \qquad \left.\frac{\partial \phi}{\partial z}\right|_{d/2} = \eta(x,y), \tag{3}$$

where $\sigma \equiv 4\pi l_B (\Sigma_B/e)$ and $\eta \equiv 4\pi l_B (\Sigma_T/e)$ are the two rescaled surface charge densities, having dimensions of inverse length. For homogeneous surface charge densities the rescaled densities σ and η are the inverse of the Gouy-Chapman length [2] (up to a factor of two) that characterizes the thickness of the condensed ionic layer near a homogeneously charged surface. The boundary conditions contain an implicit simplification that all the electric field lines are contained within the aqueous medium between the two surfaces. This commonly used assumption [39] is strictly correct in the limit where the surfaces are either infinitely thick or that the external regions have vanishing dielectric constant.

The interaction energy between the two surfaces as a function of the separation d is given by the free energy, $F(d)$, subject to the boundary conditions, Eq. (3). We obtain $F(d)$ by using the charging method [4] and calculate the work needed to increase the surface charge incrementally, at each point on the surface, from zero to the desired final value. The charging free-energy of two surfaces coupled with an ionic reservoir of density n_b is given by

$$\left(\frac{4\pi \kappa_D l_B}{k_B T}\right) F(d)$$

$$= \kappa_D \iint dx\, dy \int_{(0,0)}^{(\sigma,0)} d\sigma'\, \phi[\sigma', \eta'=0]_{z=-d/2}$$

$$+ \kappa_D \iint dx\, dy \int_{(\sigma,0)}^{(\sigma,\eta)} d\eta'\, \phi[\sigma, \eta']_{z=d/2}, \tag{4}$$

where throughout the paper $F(d)$ is made dimensionless by rescaling it, $F \rightarrow (4\pi \kappa_D l_B/k_B T)F$. The electrostatic potential on the surfaces, ϕ, is written in the above equation as a function

of the distributions σ and η to stress that the integration is performed with respect to these variables.

Equations (1)–(4) are valid for the general PB theory, while hereafter we concentrate on the linear PB equation, being valid as long as $\phi = e\psi/k_BT \ll 1$ ($\psi \ll 25$ mV):

$$\nabla^2 \phi = \kappa_D^2 \phi. \qquad (5)$$

The in-plane Fourier transform of $\phi(\boldsymbol{\rho}, z)$ in the $\boldsymbol{\rho} = (x, y)$ plane is denoted by $\phi_{\mathbf{k}}(z)$ and is given by

$$\phi_{\mathbf{k}}(z) = \int d^2\rho \, e^{i\mathbf{k}\cdot\boldsymbol{\rho}} \phi(\boldsymbol{\rho}, z), \qquad (6)$$

where $\mathbf{k}$ is the inplane wave vector. Using $\phi_{\mathbf{k}}$ we get from Eq. (5)

$$\frac{\partial^2 \phi_{\mathbf{k}}}{\partial z^2} = q^2 \phi_{\mathbf{k}}, \quad q = \sqrt{\kappa_D^2 + k^2}. \qquad (7)$$

The boundary conditions for $\phi_{\mathbf{k}}$ are similarly obtained by Fourier transforming Eq. (3):

$$\left.\frac{\partial \phi_{\mathbf{k}}}{\partial z}\right|_{-d/2} = -\sigma_{\mathbf{k}}, \quad \left.\frac{\partial \phi_{\mathbf{k}}}{\partial z}\right|_{d/2} = \eta_{\mathbf{k}}, \qquad (8)$$

where $\sigma_{\mathbf{k}}$, $\eta_{\mathbf{k}}$ are, respectively, the Fourier transforms of $\sigma(\boldsymbol{\rho})$ and $\eta(\boldsymbol{\rho})$:

$$\sigma_{\mathbf{k}} = \int d^2\rho \, e^{i\mathbf{k}\cdot\boldsymbol{\rho}} \sigma(\boldsymbol{\rho}), \quad \eta_{\mathbf{k}} = \int d^2\rho \, e^{i\mathbf{k}\cdot\boldsymbol{\rho}} \eta(\boldsymbol{\rho}). \qquad (9)$$

Solving for the z dependence of $\phi_{\mathbf{k}}$, Eqs. (7) and (8) yield

$$\phi_{\mathbf{k}}(z) = \frac{(\sigma_{\mathbf{k}} + \eta_{\mathbf{k}})\cosh(qz)}{2q\sinh(qd/2)} + \frac{(\eta_{\mathbf{k}} - \sigma_{\mathbf{k}})\sinh(qz)}{2q\cosh(qd/2)}. \qquad (10)$$

The free energy can be reexpressed in terms of the Fourier transforms $\sigma_{\mathbf{k}}$, $\eta_{\mathbf{k}}$, and $\phi_{\mathbf{k}}$. By substituting Eq. (10) into the free energy [Eq. (4)] we obtain

$$F(d)$$
$$= \kappa_D \int \frac{d^2k}{(2\pi)^2} \frac{\sigma_{\mathbf{k}}\eta_{-\mathbf{k}} + \sigma_{-\mathbf{k}}\eta_{\mathbf{k}} + (\sigma_{\mathbf{k}}\sigma_{-\mathbf{k}} + \eta_{\mathbf{k}}\eta_{-\mathbf{k}})e^{-qd}}{2q\sinh(qd)},$$
$$\qquad (11)$$

where the reference contribution at $d \to \infty$ was subtracted in order to obtain zero interaction between surfaces at infinite separation, $F(d \to \infty) = 0$. Because of the linearity, the PB free energy can also be written as a sum of two decoupled variables $\sigma_{\mathbf{k}}^{\pm} \equiv (\sigma_{\mathbf{k}} \pm \eta_{\mathbf{k}})/2$:

$$F(d) = \kappa_D \int \frac{d^2k}{(2\pi)^2} \left[\frac{e^{-qd/2}}{q\sinh(qd/2)} \sigma_{\mathbf{k}}^+ \sigma_{-\mathbf{k}}^+ \right.$$
$$\left. - \frac{e^{-qd/2}}{q\cosh(qd/2)} \sigma_{\mathbf{k}}^- \sigma_{-\mathbf{k}}^- \right]. \qquad (12)$$

The first term is positive definite and decreases monotonically as a function of the separation d, contributing to the repulsive part of the intersurface interaction, while the second term, being negative definite and a monotonic increasing function of d, gives the attractive part of the interaction.

Quite generally, it can be stated that the magnitude of the repulsive term is larger than the attractive one for all values of q and d, because of the inequality $\sinh(qd/2) < \cosh(qd/2)$. Furthermore, for $d \to 0$ the magnitude of the repulsive term

diverges, while the attractive term approaches a finite limiting value. Consequently, only when $\sigma_{\mathbf{k}}^+ \sigma_{-\mathbf{k}}^+ = 0$ for any wave number $\mathbf{k}$, does the interaction become attractive for *any* d. This occurs only when the distributions of the two surfaces are completely out-of-phase (antisymmetric) with each other, $\sigma(\boldsymbol{\rho}) = -\eta(\boldsymbol{\rho})$. Furthermore, by properly choosing $\sigma_{\mathbf{k}}^{\pm}$, $F(d)$ can be made attractive for large enough d.

III. PERIODIC SURFACE CHARGE MODULATION

In the previous section the distributions $\sigma(\boldsymbol{\rho})$ and $\eta(\boldsymbol{\rho})$ have been taken to be arbitrary. Hence, the intersurface interaction of Eqs. (11) and (12) applies to any form of surface charge distributions. We treat next two interacting charged surfaces each characterized by a periodic charge modulation. As periodic charge modulations have been investigated previously [18–26], we revisit the periodic case in order to discuss the interesting crossover from attraction to repulsion and the limiting behavior for small and large periodic domains. It is also instructive to compare the periodic case with the quenched disorder that will be derived later in Sec. IV.

A. Single mode

We first consider two surfaces characterized by the same single-$\mathbf{k}_0$ mode modulation

$$\sigma(\boldsymbol{\rho}) = C_\sigma \cos(\mathbf{k}_0 \cdot \boldsymbol{\rho}), \quad \eta(\boldsymbol{\rho}) = C_\eta \cos(\mathbf{k}_0 \cdot \boldsymbol{\rho} + \varphi), \qquad (13)$$

where C_σ and C_η (having units of inverse length) are the modulation amplitudes of the two surfaces, taken to be positive without loss of generality. The angle $-\pi \leqslant \varphi \leqslant \pi$ is the relative phase between the two charge modulations. It reflects an in-phase arrangement of like charges at $\varphi = 0$, and an antiphase one at $\varphi = \pm\pi$.

The intersurface interaction per unit area, $F(d)/A$, is given by

$$\frac{F(d)}{A} = \frac{2\kappa_D C_\sigma C_\eta \cos\varphi + \kappa_D e^{-q_0 d}(C_\sigma^2 + C_\eta^2)}{4q_0 \sinh(q_0 d)}, \qquad (14)$$

where A is the lateral surface area and $q_0 = \sqrt{\kappa_D^2 + k_0^2}$. For large separations, $q_0 d \gg 1$, the energy decays exponentially, $F/A \sim \kappa_D q_0^{-1} e^{-q_0 d}$, while for small separations, $q_0 d \ll 1$, the energy scales as $F/A \sim \kappa_D (q_0^2 d)^{-1}$. We note that at sufficiently small separations, where the linearized PB equation is not valid, the scaling of the free energy should be $F \sim \log d$ as obtained from the nonlinear PB equation for homogeneously charged surfaces.

Rewriting F/A in terms of $C_\pm \equiv (C_\sigma \pm C_\eta)/2$ as in Eq. (12) leads to

$$\frac{F(d)}{A} = \frac{\kappa_D}{2q_0} \frac{e^{-q_0 d} + \cos\varphi}{\sinh(q_0 d)} C_+^2 + \frac{\kappa_D}{2q_0} \frac{e^{-q_0 d} - \cos\varphi}{\sinh(q_0 d)} C_-^2. \qquad (15)$$

Here both the C_+^2 and C_-^2 terms can be either repulsive or attractive, depending on the values of d and φ.

In Fig. 2 the intersurface interaction per unit area $F(d)/A$ is presented for charge modulations with two equal amplitudes, $C_\sigma = C_\eta = C_+$. The second term of Eq. (15) then vanishes as $C_- = 0$, and the sign of the interaction energy is determined
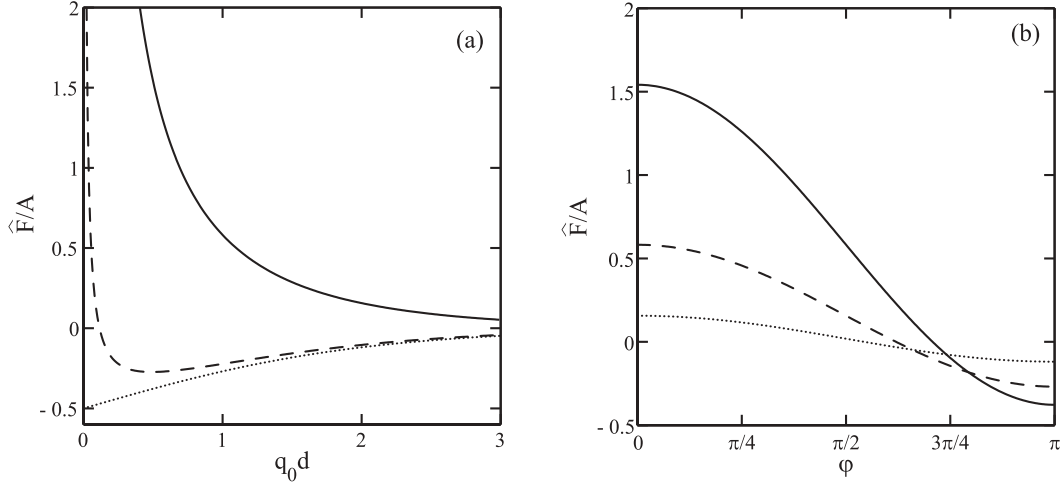
FIG. 2. The intersurface interaction (per unit area) $\widehat{F}/A$ for a single q_0 mode, rescaled by the prefactor of Eq. (15), $\widehat{F} = (q_0/\kappa_{\rm D}C_+^2)F$, and plotted for the equal amplitude case: $C_\sigma = C_\eta = C_+$ ($C_- = 0$). (a) The intersurface interaction as a function of the intersurface separation d in units of q_0^{-1}. The values of the relative angle φ are 0, 0.85π, π for the solid, dashed, and dotted lines, respectively. (b) The intersurface interaction as a function of the relative phase φ. The values of q_0d are 0.5, 1, and 2 for the solid, dashed, and dotted lines, respectively.

by the relative phase φ and d. The repulsion is maximal with respect to φ for the in-phase state $\varphi = 0$, while for the antiphase state, $\varphi = \pm\pi$, the attraction is maximal:

$$\frac{F(d)}{A} = \begin{cases} \dfrac{\kappa_{\rm D}}{2q_0}\dfrac{{\rm e}^{-q_0d/2}}{\sinh(q_0d/2)}C_+^2 & \text{for} \quad \varphi = 0 \\[3mm] -\dfrac{\kappa_{\rm D}}{2q_0}\dfrac{{\rm e}^{-q_0d/2}}{\cosh(q_0d/2)}C_+^2 & \text{for} \quad \varphi = \pm\pi \end{cases}. \quad (16)$$

Furthermore, for modulated surfaces with equal amplitudes, $C_\sigma = C_\eta$, the interaction in Eq. (15) is purely repulsive in the range $|\varphi| < \pi/2$, where the cosine is positive. When $\cos\varphi$ becomes negative, in the range $\pi/2 < |\varphi| < \pi$, the intersurface interaction $F(d)$ has a minimum at $d_c = q_0^{-1}\cosh^{-1}(1/|\cos\varphi|)$, leading to a crossover from attraction for $d > d_c$ to repulsion for $d < d_c$.

The interaction between two non-neutral and uniformly charged surfaces is obtained by setting $\mathbf{k}_0 = \varphi = 0$ in Eqs. (12) and (13), recovering the well-known result of Parsegian and Gingell [40]:

$$\frac{F(d)}{A} = \frac{{\rm e}^{-\kappa_{\rm D}d/2}}{\sinh(\kappa_{\rm D}d/2)}C_+^2 - \frac{{\rm e}^{-\kappa_{\rm D}d/2}}{\cosh(\kappa_{\rm D}d/2)}C_-^2, \quad (17)$$

written here in a decoupled way, separating the pure repulsive from the pure attractive contributions in terms of the amplitudes $C_\pm = (C_\sigma \pm C_\eta)/2$, where C_σ and C_η are uniform surface charge densities. Unlike neutral modulated surfaces, for two uniformly charged surfaces with the same sign ($C_\sigma \cdot C_\eta > 0$), the interaction is purely repulsive since the inequality $C_+ > C_-$ is always valid.

For uniform charged surfaces, only the ions in solution screen the interaction, whereas for modulated charged surfaces there is an additional screening effect, yielding an effective screening length, $q_0^{-1} = 1/\sqrt{\kappa_{\rm D}^2 + k_0^2}$. Therefore, the lateral charge modulations result in a faster decay of the interaction as compared to the interaction between two uniformly charged surfaces, due to the additional mechanism of screening.

Note that when two surfaces have each a different single-mode modulation, $k_\sigma \neq k_\eta$, the integral over the coupling terms in Eq. (11) vanishes, leading to a purely repulsive interaction:

$$\frac{F(d)}{A} = \frac{\kappa_{\rm D}}{4q_\sigma}\frac{{\rm e}^{-q_\sigma d}}{\sinh(q_\sigma d)}C_\sigma^2 + \frac{\kappa_{\rm D}}{4q_\eta}\frac{{\rm e}^{-q_\eta d}}{\sinh(q_\eta d)}C_\eta^2, \quad (18)$$

where $q_\sigma = \sqrt{\kappa_{\rm D}^2 + k_\sigma^2}$, $q_\eta = \sqrt{\kappa_{\rm D}^2 + k_\eta^2}$, and k_σ, k_η are the wave numbers of the bottom and top surfaces, respectively.

The intersurface interaction as expressed in Eq. (18) can be interpreted as a superposition of two decoupled systems each composed of one uniform charged surface and a second (virtual) surface that is neutral. Namely, the first term corresponds to a uniformly charged surface located at $z = -d/2$ and a neutral one located at $z = +d/2$, while the second term corresponds to a neutral surface located at $z = -d/2$ and a uniformly charged surface located at $z = +d/2$. Although the *virtual* surface is neutral and does not interact electrostatically, it leads to a repulsive interaction because the counter-ions are confined between the two surfaces and their translational entropy is reduced. The magnitude of the confined ionic volume depends linearly on d and decreases at smaller separations.

The above result suggests that a slight difference between the two wavelengths ($k_\sigma \neq k_\eta$) is sufficient to eliminate any intersurface attraction between two periodically ordered surfaces, implying that the attraction is a delicate effect that might be difficult to obtain in experimental conditions corresponding to the linear PB regime.

B. Multimode modulation

The analysis of the previous section can be generalized to multimode distributions of the charges on the two surfaces. The charge distributions are written as

$$\sigma(\boldsymbol{\rho}) = \delta\sigma(\boldsymbol{\rho}) + \sigma_0, \quad \eta(\boldsymbol{\rho}) = \delta\eta(\boldsymbol{\rho}) + \eta_0, \quad (19)$$

where $\sigma_0 = \langle \sigma \rangle$ and $\eta_0 = \langle \eta \rangle$ are the average surface charge densities, and $\delta\sigma(\boldsymbol{\rho})$ and $\delta\eta(\boldsymbol{\rho})$ are the charge modulations around these averages. The intersurface interaction of Eq. (11) can be separated into two terms:

$$F(d) = F_0(d) + F_1(d), \qquad (20)$$

where the first term depends only on σ_0 and η_0, and coincides with Eq. (17) with $C_\pm = (\sigma_0 \pm \eta_0)/2$:

$$\frac{F_0(d)}{A} = \frac{2\sigma_0\eta_0 + (\sigma_0^2 + \eta_0^2)\, e^{-\kappa_{\mathrm{D}} d}}{2\sinh(\kappa_{\mathrm{D}} d)}. \qquad (21)$$

It vanishes when both surfaces are neutral, $\sigma_0 = \eta_0 = 0$. The second term is the contribution due to charge heterogeneity, given by Eq. (11) without the mode $\mathbf{k} = 0$:

$$F_1(d) = \kappa_{\mathrm{D}} \int \frac{d^2k}{(2\pi)^2} \left[\frac{\delta\sigma_{\mathbf{k}}\delta\eta_{-\mathbf{k}} + \delta\sigma_{-\mathbf{k}}\delta\eta_{\mathbf{k}}}{2q\sinh(qd)} \right.$$
$$\left. + \frac{(\delta\sigma_{\mathbf{k}}\delta\sigma_{-\mathbf{k}} + \delta\eta_{\mathbf{k}}\delta\eta_{-\mathbf{k}})e^{-qd}}{2q\sinh(qd)} \right], \qquad (22)$$

where $\delta\sigma_{\mathbf{k}}$ and $\delta\eta_{\mathbf{k}}$ are the Fourier transforms of $\delta\sigma(\boldsymbol{\rho})$ and $\delta\eta(\boldsymbol{\rho})$, respectively. By definition, from Eq. (19), $\langle\delta\sigma\rangle = \langle\delta\eta\rangle = 0$, or equivalently in Fourier space $\delta\sigma_{\mathbf{k}=0} = \delta\eta_{\mathbf{k}=0} = 0$. Note that $\delta\sigma_{\mathbf{k}}$ and $\delta\eta_{\mathbf{k}}$ have units of length in Fourier space (unlike the units of C_σ and C_η). Hence, F_1 is dimensionless.

An important length scale for a general periodic (multimode) distribution is the periodic charged domain size, L, which is related to the smallest wave number, $L = 2\pi/k_{\min}$. The wave vector $\mathbf{k}_{\min}$ also acts as a lower cutoff in the $\mathbf{k}$-space integration, Eq. (22).

Two limiting cases of small and large $k_{\min}$ can be considered separately. In the limit of charges with molecular-size heterogeneities, the domain size is molecular $L \ll \kappa_{\mathrm{D}}^{-1}$, and $q_{\min} = \sqrt{\kappa_{\mathrm{D}}^2 + k_{\min}^2} \simeq 2\pi/L \gg \kappa_{\mathrm{D}}$ depends inversely on L. Therefore, the leading term in the integrand varies as $\kappa_{\mathrm{D}} q^{-1} e^{-qd} \simeq \kappa_{\mathrm{D}} L e^{-2\pi d/L} \to 0$ (as long as $L \ll d$) and leads to a negligible contribution due to charge heterogeneity, $F_1(d) \to 0$.

On the other hand, in the limit of large domains, $L \gg \kappa_{\mathrm{D}}^{-1}$, $q_{\min} \simeq \kappa_{\mathrm{D}} + O(L^{-2})$ has no dependence on L. The decay length of the interaction is the Debye length, κ_{D}^{-1}, similarly to the average charge contribution in Eq. (21). The leading term of $F_1(d)$ is then given by

$$F_1(d) \simeq \frac{S_1 + S_2 e^{-\kappa_{\mathrm{D}} d}}{\sinh(\kappa_{\mathrm{D}} d)}, \qquad (23)$$

where the prefactors $S_1 = \frac{1}{2}\int \frac{d^2k}{(2\pi)^2}(\delta\sigma_{\mathbf{k}}\delta\eta_{-\mathbf{k}} + \delta\sigma_{-\mathbf{k}}\delta\eta_{\mathbf{k}})$, and $S_2 = \frac{1}{2}\int \frac{d^2k}{(2\pi)^2}(|\delta\sigma_{\mathbf{k}}|^2 + |\delta\eta_{\mathbf{k}}|^2) > 0$ do not depend on d and can be interpreted as contributions from effective uniform surface charges.

The similar dependence on d of Eqs. (21) and (23) implies that the effect of large domains can be understood as a modification of the prefactors in Eq. (21). When S_1 is negative, the contribution $F_1(d) \simeq 2S_1 e^{-\kappa_{\mathrm{D}} d} < 0$ is attractive for large separations $\kappa_{\mathrm{D}} d \gg 1$ and is followed by a crossover at $d_c = \kappa_{\mathrm{D}}^{-1}\cosh^{-1}(-S_2/S_1)$ from attraction for $d > d_c$ to repulsion for $d < d_c$, resembling the crossover found in Eq. (15).

Examining the two limits of small and large domains leads to the observation that periodic charge modulation has a

significant effect only when the domain size is sufficiently large. Thus, for charge modulations characterized by molecular heterogeneities, one can treat the interaction effectively as if the charges on the two surfaces are distributed homogeneously. On the other hand, for surfaces where the charged domains are larger than the Debye screening length κ_{D}^{-1}, the contribution due to charge modulation cannot be neglected and may lead to a substantial change in the strength of the intersurface interaction. Furthermore, a crossover from repulsion at $d < d_c$ to attraction at larger separations, $d > d_c$, can be induced.

C. Time-dependent lateral displacement and intersurface correlations

The case of two identical single-mode distributions with a relative phase φ, Eqs. (13)–(15), can be generalized for two identical multimode distributions with a relative lateral displacement $\boldsymbol{\ell}$:

$$\delta\eta(\boldsymbol{\rho} + \boldsymbol{\ell}) = \delta\sigma(\boldsymbol{\rho}). \qquad (24)$$

The above charge distribution, Eq. (24), is motivated by a specific intersurface force experiment setup [15] that will be discussed in Sec. V, while here we explore its theoretical consequences. The relative displacement $\boldsymbol{\ell} = (\ell_x, \ell_y)$ is related to a k-dependent phase $\varphi_{\mathbf{k}} = \mathbf{k} \cdot \boldsymbol{\ell}$ in Fourier space with $\delta\eta_{\mathbf{k}} = \delta\sigma_{\mathbf{k}}e^{i\varphi_{\mathbf{k}}}$, and F_1 from Eq. (22) reads

$$F_1(d) = \kappa_{\mathrm{D}} \int \frac{d^2k}{(2\pi)^2} \frac{\cos(\mathbf{k}\cdot\boldsymbol{\ell}) + e^{-qd}}{q\sinh(qd)} |\delta\sigma_{\mathbf{k}}|^2. \qquad (25)$$

For $\boldsymbol{\ell} = 0$ the two distributions are in-phase (symmetric), leading to repulsive contributions from all modes for any d. In the more general case of a relative displacement $\boldsymbol{\ell} \neq 0$, each $\mathbf{k}$ mode can have either an attractive or a repulsive contribution, and Eq. (25) gives the overall positive or negative sign of F_1, due to strong correlations between the two surfaces.

We consider two surfaces with identical charge distributions that are relatively displaced by applying on one of them a time-dependent lateral force. This force leads to a time-dependent lateral vector $\boldsymbol{\ell}(t)$ such that $\delta\eta[\boldsymbol{\rho} + \boldsymbol{\ell}(t)] = \delta\sigma(\boldsymbol{\rho})$. The time dependence $\boldsymbol{\ell}(t)$ is related to the temporal dependence of the applied lateral (shear) force. The validity of this model holds as long as the lateral motion is a quasistatic process, for which the ions in the solution equilibrate faster than the typical time scale of the surface lateral motion. Then, the intersurface interaction is given by averaging the $\cos[\mathbf{k} \cdot \boldsymbol{\ell}(t)]$ term in Eq. (25) over the displacement period T:

$$\langle F_1(d) \rangle_T = \kappa_{\mathrm{D}} \int \frac{d^2k}{(2\pi)^2} \frac{\langle\cos[\mathbf{k}\cdot\boldsymbol{\ell}(t)]\rangle_T + e^{-qd}}{q\sinh(qd)} |\delta\sigma_{\mathbf{k}}|^2, \qquad (26)$$

where F_1 is the contribution to the intersurface interaction due to charge modulation, and $\langle O \rangle_T = T^{-1}\int_0^T dt\, O(t)$ is the time average. Since the average of the cosine depends on the lateral periodic motion, the interaction energy would vary when changing the oscillatory mode of the force.

A simple example is a square-wave motion in the $\hat{x}$ direction, given by

$$\boldsymbol{\ell}(0 < t < T) = \begin{cases} (\ell_0 - \Delta\ell)\hat{x} & 0 < t \leqslant T/2, \\ (\ell_0 + \Delta\ell)\hat{x} & T/2 < t \leqslant T, \end{cases} \qquad (27)$$

where ℓ_0 is the mean lateral displacement between the two surfaces, and $\Delta\ell$ is the oscillation amplitude. The intersurface interaction is given by

$$\langle F_1(d)\rangle_T$$
$$= \kappa_{\rm D} \int \frac{d^2k}{(2\pi)^2} \frac{\cos(k_x\ell_0)\cos(k_x\Delta\ell) + e^{-qd}}{q\,\sinh(qd)} |\delta\sigma_{\bf k}|^2, \quad (28)$$

and depends both on the mean displacement ℓ_0 and the oscillation amplitude $\Delta\ell$. Here k_x is the wave-vector component along the direction of the shear motion.

For a general periodic dependence $\ell(t)$, if the amplitude of the lateral oscillations $\Delta\ell(t) = \ell(t) - \ell_0$ is small, $k_x\Delta\ell \ll 1$, and to leading orders the interaction depends on the average displacement, ℓ_0, and the mean square amplitude of the oscillation, $\langle\Delta\ell^2\rangle_T = \Delta\ell^2$:

$$\langle F_1(d)\rangle_T \simeq \kappa_{\rm D} \int \frac{d^2k}{(2\pi)^2} \left[\frac{\left(1 - \frac{1}{2}k_x^2(\Delta\ell)^2\right)\cos(k_x\ell_0)}{q\,\sinh(qd)} \right.$$
$$\left. + \frac{e^{-qd}}{q\,\sinh(qd)} \right] |\delta\sigma_{\bf k}|^2. \quad (29)$$

Note that the above equation is exact for the square-wave distribution of Eq. (27).

IV. QUENCHED SURFACE DISORDER: PATCHY SURFACES

We generalize now the periodic distribution of Sec. III to patchy surfaces with random charged domains, but which are overall neutral. Consider two surfaces with charge distributions $\sigma(\boldsymbol{\rho})$ and $\eta(\boldsymbol{\rho})$, respectively. The surface charges are randomly distributed with a joint probability distribution $P[\sigma(\boldsymbol{\rho}),\eta(\boldsymbol{\rho})]$. The intersurface interaction, Eq. (11), is obtained by averaging over the bilinear terms of the Fourier transform:

$$\langle F(d)\rangle_{\sigma,\eta} = \kappa_{\rm D} \int \frac{d^2k}{(2\pi)^2} \left[\frac{\langle\sigma_{\bf k}\eta_{-\bf k}\rangle_{\sigma,\eta} + \langle\sigma_{-\bf k}\eta_{\bf k}\rangle_{\sigma,\eta}}{2q\,\sinh(qd)} \right.$$
$$\left. + \frac{\langle\sigma_{\bf k}\sigma_{-\bf k}\rangle_{\sigma,\eta} + \langle\eta_{\bf k}\eta_{-\bf k}\rangle_{\sigma,\eta}}{2q\,\sinh(qd)} e^{-qd} \right], \quad (30)$$

where $\langle O\rangle_{\sigma,\eta} = \int \mathcal{D}\sigma \int \mathcal{D}\eta\, P[\sigma,\eta]\, O$ is the average over the joint σ and η distribution. In experiments the probability distribution is usually determined by the preparation procedure of the surfaces.

When the surfaces are prepared separately, there are no intersurface correlations, $\langle\sigma_{\bf k}\eta_{-\bf k}\rangle = 0$, leading to a purely repulsive interaction:

$$\langle F(d)\rangle_{\sigma,\eta}$$
$$= \kappa_{\rm D} \int \frac{d^2k}{(2\pi)^2} \frac{\langle\sigma_{\bf k}\sigma_{-\bf k}\rangle_\sigma + \langle\eta_{\bf k}\eta_{-\bf k}\rangle_\eta}{2q\,\sinh(qd)} e^{-qd} > 0, \quad (31)$$

and the strength of the repulsive interaction depends on the probability distribution of each surface. For an uncorrelated Gaussian distribution, the two-point correlation function is given by

$$\langle\sigma(\boldsymbol{\rho})\sigma(\boldsymbol{\rho}')\rangle_\sigma = \langle\eta(\boldsymbol{\rho})\eta(\boldsymbol{\rho}')\rangle_\eta = \gamma^2 \delta\left(\frac{\boldsymbol{\rho} - \boldsymbol{\rho}'}{a}\right), \quad (32)$$

where $\delta(\boldsymbol{\rho})$ is the two-dimensional Dirac δ-function, γ is the root mean square charge density (taken to be the same on the two surfaces), and a is a conveniently defined molecular length. This leads to $\langle\sigma_{\bf k}\sigma_{-\bf k}\rangle_\sigma = \langle\eta_{\bf k}\eta_{-\bf k}\rangle_\eta = A\gamma^2 a^2$, and to an intersurface interaction per unit area:

$$\frac{\langle F(d)\rangle_{\sigma,\eta}}{A} = \frac{\kappa_{\rm D}^2 \gamma^2 a^2}{2\pi} I(\kappa_{\rm D}d) > 0, \quad (33)$$

where

$$I(\kappa_{\rm D}d) = \int_0^\infty dk \frac{k e^{-qd}}{\kappa_{\rm D} q\,\sinh(qd)} = -\frac{\ln(1 - e^{-2\kappa_{\rm D}d})}{\kappa_{\rm D}d}. \quad (34)$$

The repulsive free energy for the uncorrelated Gaussian case is presented in Fig. 3(a). At separations larger than the Debye screening length, $\kappa_{\rm D}d \gg 1$, the leading term decays exponentially as $\langle F\rangle/A \sim e^{-2\kappa_{\rm D}d}/(\kappa_{\rm D}d)$, while at small separations, $\kappa_{\rm D}d \ll 1$, the energy scales as $\langle F\rangle/A \sim \ln[1/(2\kappa_{\rm D}d)]/(\kappa_{\rm D}d)$.

When calculating these scaling relations we ignored the molecular length scale a, since $I(\kappa_{\rm D}d)$ has no dependence on a. However, the prefactor in Eq. (33) scales as the square of the molecular length scale $\langle F\rangle/A \sim (\kappa_{\rm D}a)^2$. Hence, the contribution of uncorrelated Gaussian disorder, Eq. (32), vanishes in the limit where a is much smaller than the Debye length, $\kappa_{\rm D}a \ll 1$, in agreement with the results reported in Ref. [37].

In order to model the possibility of finite (macroscopic) charged domains we replace Eq. (32) by a two-point correlation function having a Lorentzian distribution:

$$\langle\sigma(\boldsymbol{\rho})\sigma(\boldsymbol{\rho}')\rangle_\sigma = \langle\eta(\boldsymbol{\rho})\eta(\boldsymbol{\rho}')\rangle_\eta = \frac{\gamma^2\xi^2}{(\boldsymbol{\rho} - \boldsymbol{\rho}')^2 + \xi^2}, \quad (35)$$

where ξ is the charge correlation length on the surface, which can be associated with the domain size. In Fourier space this leads to $\langle\sigma_{\bf k}\sigma_{-\bf k}\rangle_\sigma = \langle\eta_{\bf k}\eta_{-\bf k}\rangle_\eta = 2\pi A\gamma^2\xi^2 K_0(k\xi)$, where $K_0(x)$ is the zeroth-order modified Bessel function of the second kind.

The intersurface interaction is then given by

$$\frac{\langle F(d)\rangle_{\sigma,\eta}}{A} = \kappa_{\rm D}\gamma^2\xi^2 \int_0^\infty dk \frac{k e^{-qd} K_0(k\xi)}{q\,\sinh(qd)}, \quad (36)$$

and the dependence of $\langle F(d)\rangle_{\sigma,\eta}$ on $\kappa_{\rm D}d$ for three values of the correlation length ξ is shown in Fig. 3(b). In the limit of short-range correlations [dotted line in Fig. 3(b)], $\kappa_{\rm D}\xi \ll 1$, the integrand in Eq. (36) depends weakly on ξ, and the interaction energy scales as $\langle F\rangle/A \sim -\ln(\kappa_{\rm D}\xi)\xi^2$, resembling the scaling of the Gaussian distribution case, Eq. (33), where $\langle F\rangle \sim a^2$. In the other limit of large domains [solid line in Fig. 3(b)], where $\kappa_{\rm D}\xi \gg 1$, the main contribution to the integral comes from the small values of k, and the interaction is independent of ξ, $\langle F\rangle/A \sim e^{-\kappa_{\rm D}d}/\sinh(\kappa_{\rm D}d)$. This reproduces repulsion with a decay length that does not depend on the lateral length scale, ξ. These two limiting behaviors of $\langle F\rangle/A$ as a function of $\kappa_{\rm D}\xi$ are shown in the inset of Fig. 3(b) for two values of d.

By examining the short- and long-range charge distributions we find that short-range charge disorder has a negligible effect on the intersurface energy, while long-range disorder leads to a substantial effect, which cannot be omitted even in the case of nonzero average charge. This observation is in accord with the results presented in the multimode periodic case, Sec. III B, where it was found that charge distributions with large charge domains changed the intersurface interaction substantially,
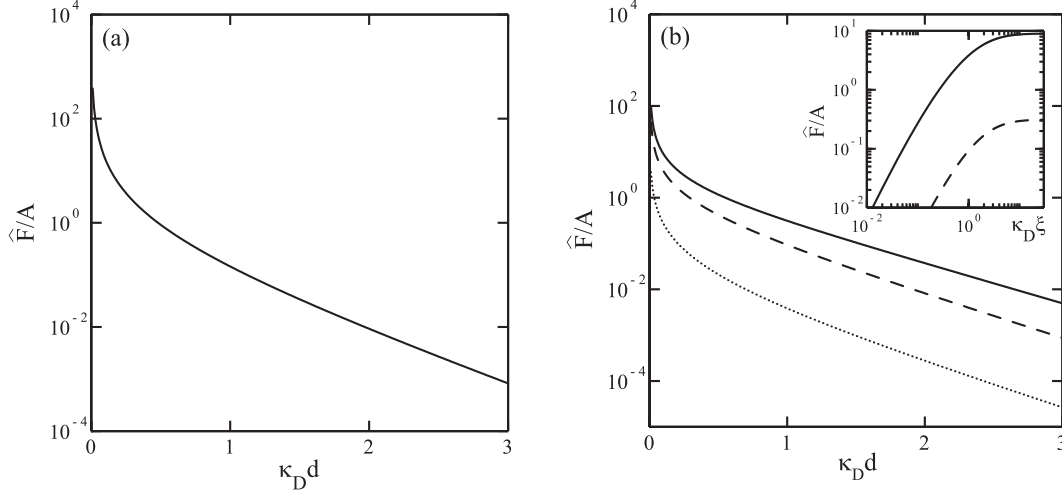
FIG. 3. The averaged interaction energy, $\widehat{F}/A$ as a function of the intersurface separation d for randomly charged surfaces. (a) The free energy from Eq. (33), for an uncorrelated Gaussian distribution [Eq. (32)], is plotted on a semilog plot as a function of $\kappa_D d$. (b) The free energy is plotted on a semilog plot as a function of $\kappa_D d$, where the charge distribution is a two-dimensional Lorentzian, Eq. (36). Three values of $\kappa_D \xi$ are shown: $\kappa_D \xi = 100$ (solid line), $\kappa_D \xi = 1$ (dashed line), and $\kappa_D \xi = 0.1$ (dotted line). In the inset the dependence of the free energy on $\kappa_D \xi$ is plotted on a log-log scale for two values of the separation: $\kappa_D d = 0.1$ (solid line) and $\kappa_D d = 1$ (dashed line). The plotted free energy is rescaled by the prefactor of Eq. (33), $\widehat{F} = 2\pi \langle F \rangle / (\kappa_D^2 \gamma^2 a^2)$ for (a), and $\widehat{F} = \langle F \rangle / \gamma^2$ from Eq. (36) for (b).

while distributions with small domains lead to a negligible effect.

V. DISCUSSION

The model we present accounts for the intersurface interaction of two heterogeneously charged surfaces. It is formulated on the mean-field level where the electrostatic potential is given by the Poisson-Boltzmann (PB) equation. Our main aim is to study the effect of quenched charge disorder with finite domains on the intersurface interaction between the two surfaces.

We focus on the linear regime of the PB equation, where it is found that the intersurface interaction of two arbitrary charge distributions depends on a bilinear coupling between the Fourier components of the two distributions. It is shown that the interaction can be expressed as a sum of an attractive term and a repulsive one. The repulsive term at small separations is usually larger than the attractive one, leading to a repulsion for $d \to 0$. In a special case where the two distributions are exactly out-of-phase, $\sigma(\boldsymbol{\rho}) = -\eta(\boldsymbol{\rho})$, such that negatively charged domains are located against positively charged domains in the other surface and vice versa, the interaction is attractive for any value of d.

Several types of surface charge distributions are studied in the linear PB regime. First, we consider two overall neutral surfaces with the same single-mode periodic charge density, but with a relative phase shift φ between the two. When the average surface charge is taken to be zero, the intersurface interaction stems only from the lateral charge modulation. When the top surface mode is identical with the bottom one, the interaction can vary between pure attraction and pure repulsion as function of the relative phase φ between the two surfaces. For an out-of-phase distribution, $\varphi = \pi$, there is a relative displacement by half a wavelength between the bottom and top surfaces, and the interaction is purely attractive, while for the in-phase case, $\varphi = 0$, it is purely repulsive.

These two limits are a consequence of strong intersurface correlations. For intermediate values of the relative phase φ, the correlation is weaker and a crossover from attraction (at large separations) to repulsion (at small separations) occurs at a separation $d_c \sim \cosh^{-1}(1/|\cos \varphi|)$. Note that the crossover separation d_c does not depend on the modulation amplitude. In the more general case where the bottom and top surfaces have different (single) k mode, the interaction is found to be purely repulsive. The origin of the repulsion in this case is due to the confinement of the counter-ions in between the surfaces.

The role of the domain size in a general periodic (multimode) distribution is also investigated. It is found that the contribution due to periodic charge modulation is important only in the limit of large domains $\kappa_D L \gg 1$. For sufficiently large domains the contribution due to charge heterogeneity is substantial, even in the case of non-neutral surfaces, where the main contribution stems from the average surface charge.

The time-dependent relative displacement case discussed in Sec. III C is motivated by a recent surface force experiment [15], which examined whether the charge heterogeneity on the two surfaces is annealed or randomly distributed (quenched case). In the experiments, the normal forces between two mica surfaces partially coated with a cationic lipid bilayer were measured, while during the vertical approach the surfaces were also sheared laterally in an oscillatory mode at a rate which is slower than the typical time required for the ions in solution to rearrange, but faster than the time scale of vertical approach or lipids rearrangement on the coated surfaces. Thus, it is assumed that the initial ordering of the surface charge on each surface is preserved during the normal approach.

If the hypothesis that the surfaces are periodically ordered [34] is correct, then the measured intersurface force should depend on the average and mean square amplitude of the lateral motion as in Eqs. (28) and (29). However, it was shown in Ref. [15] that the forces measured for different lateral

motions remained unchanged, suggesting that the surface charge distribution is not periodic, but presumably is quenched and random.

While in the annealed case the surface charges can rearrange themselves, and the system approaches the minimum energy state as was investigated in Refs. [33–36], in the quenched case the accessible configurations of the surfaces are frozen. The quenched probability distribution is usually determined by the experimental setup. For example, in surface force experiments the two surfaces are prepared separately before the force measurement, and their corresponding charge distributions can be assumed to be independent with no intersurface correlation. We consider this case and find that the interaction is purely repulsive in the linear PB model, due to the vanishing of intersurface bilinear coupling terms. The intersurface interaction can be thought of as an average over equal weights of repulsive and attractive contributions. However, since the repulsive term varies as $\exp(-qd/2)/\sinh(qd/2)$ and the attractive one as $\exp(-qd/2)/\cosh(qd/2)$, the repulsive contribution is always larger than the attractive one, leading to an overall repulsive interaction between uncorrelated randomly charged surfaces in the linear PB model.

We discuss two specific types of random distributions. For Gaussian charge distributions with no inter- and intrasurface correlations, the interaction depends on a molecular length scale a (lower cutoff length). Disorder at the molecular level may emerge due to local processes that are not affected by neighboring surface charges. The contribution of the heterogeneity in this case is negligible, in agreement with Ref. [37].

In a more general case of Lorentzian distribution with correlation length ξ, we find two limiting regimes. For large values of ξ we obtain a substantial effect due to charge disorder, while for small values of ξ the limit of disorder at the molecular level is recovered and the contribution due to disorder is negligible. Note the similarity between these two limiting regimes and the case of periodic distributions mentioned earlier. For the latter and in the limit of large domains, $\kappa_\mathrm{D} L \gg 1$, the effect is significant, while in the small domain limit, $\kappa_\mathrm{D} L \ll 1$, the domain-size effect is quite negligible.

All the results obtained in the present work assumed a linear PB regime and demonstrate that quenched charge disorder leads (except in special setups) to a nonvanishing repulsive interaction between charged surfaces. It is reasonable to expect that similar considerations can be extended to the nonlinear PB regime, where the electrostatic potential is too large for the linear approximation to be valid. However, using a simplified model for the limit of infinitely large charged domains, it was shown in Ref. [15] that the intersurface interaction in the nonlinear regime may become overall attractive.

In the Appendix we reproduce this simplified treatment and compare its results, for a range of surface charge densities, with those of the linear model presented above. For weakly charged surfaces, when the validity of the linear PB approximation can be justified, the overall repulsion predicted in the linear regime agrees with the nonlinear one, while for strongly charged surfaces the linear PB equation fails to predict the attraction obtained in the nonlinear regime. This suggests a possible crossover from repulsive to attractive intersurface interaction, as a function of charge density and patch size.

VI. CONCLUDING REMARKS

The results presented in our work demonstrate that charge heterogeneity may have important implications on the intersurface interaction both for periodically modulated surfaces and randomly quenched ones. Several extensions to our work can be considered.

An effect not taken into account in the present work and left for future investigations is that the membrane charge distribution in reality is not planar. It is actually a three-dimensional landscape with peaks and valleys, created, for example, by the lipidic charged domains. This would result in a z-dependent charge distribution of a nano-scale thickness, hence, adding another length scale of inhomogeneity, in addition to the transverse correlation length of the planar model.

A further remark should be made on the divergence of the free energy at small separations. This is related to our simplifying assumption on the boundary conditions, Eq. (3), in which the electrostatic field is confined in between the surfaces, and does not leak to the outer region. Namely, the electrostatic field in the outward direction of the surface is set to zero. This assumption is reasonable when the dielectric constant of the outer region is much lower than the one of the ionic solution. However, for sufficiently small intersurface separations, one might need to consider the leakage of the field to the outer region [38].

Since the attraction in the nonlinear regime was predicted only in the limit of infinitely-large surface patches [15], it is worthwhile to investigate further the nonlinear PB model. It will be of interest to study the origin of the attraction and relate it to the difference between the scaling of the counter-ion entropy for counter-ion release (attraction) versus counter-ion confinement (repulsion).

Another possible extension would be to find a suitable approximation for the nonlinear PB regime in three dimensions with heterogeneous boundary conditions. Using such an approximation may shed more light on the interaction between randomly charged surfaces within the PB theory and related experiments.

APPENDIX: COMPARISON OF THE LINEAR AND NONLINEAR PB THEORY FOR INFINITELY LARGE CHARGED DOMAINS

We repeat here the calculation presented in Ref. [15] for the nonlinear PB theory and compare it with the linear theory treated in our paper. We consider two heterogeneous surfaces where the typical size of a charged patch (domain) is much larger than any other length scale in the system. Each patch can be treated as an extended section of a uniform charged surface, and the leading interaction term would presumably be a superposition of all patch-patch interactions between the two surfaces.
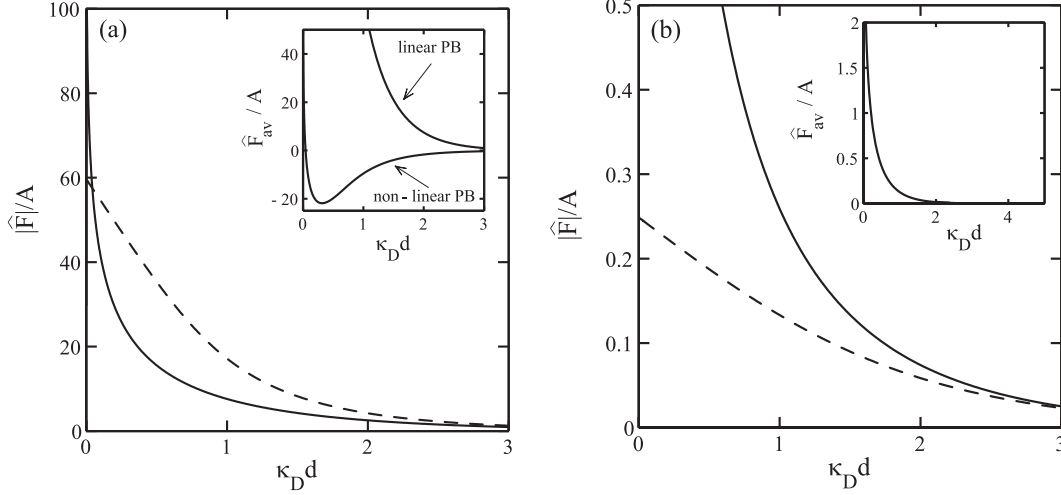
FIG. 4. The patch-patch intersurface interaction energy per unit area, $|\widehat{F}|/A$, as a function of the separation d rescaled by κ_D. The plotted free energy $\widehat{F} = F/\kappa_D^2$ is rescaled by κ_D^2. (a) Attraction $|\widehat{F}_{att}|$ (dashed line) and repulsion $\widehat{F}_{rep}$ (solid line) are calculated by the nonlinear PB equation for $\sigma = -\eta = 10\kappa_D$ and $\sigma = \eta = 10\kappa_D$, respectively. The inset shows the average of the repulsive and attractive corresponding free energies $\widehat{F}_{av} = (\widehat{F}_{rep} - |\widehat{F}_{att}|)/2$, calculated by the linear and nonlinear PB equation. (b) The solid and dashed lines are calculated with the nonlinear PB equation for $\sigma = \eta = 0.5\kappa_D$ and $\sigma = -\eta = 0.5\kappa_D$, respectively. The inset shows the average $\widehat{F}_{av}$. The results of the linear PB equation are omitted in (b) since their difference from the nonlinear calculation is invisible.

The two surfaces are overall neutral, and on each of them there are positively and negatively charged patches, with uniform charge densities: $\sigma = \eta = \pm\sigma_0$, leading to four types of possible patch-patch interactions between the two surfaces, $(\pm\sigma_0, \pm\sigma_0)$. The electrostatic potential ψ is obtained by solving numerically the nonlinear PB equation for two uniformly charged surfaces. The patch-patch interaction energy is repulsive for the like-charge case, $F_{rep} > 0$, and attractive for the opposite-charge case, $F_{att} < 0$, and is obtained by integrating over the osmotic pressure $\Pi(d)$,

$$F/A = \frac{4\pi\kappa_D l_B}{k_B T} \int_d^\infty dz\, \Pi(z), \qquad (A1)$$

where the osmotic pressure is given by

$$\Pi = -\frac{\varepsilon}{8\pi}\left(\frac{d\psi}{dz}\right)^2 + 2k_B T n_b \left[\cosh\left(\frac{e\psi}{k_B T}\right) - 1\right] \qquad (A2)$$

and has the same dependence on ψ for both attractive and repulsive cases. The overall free energy F_{av} is then given by averaging over the four possible patch-patch arrangements, yielding $F_{av} = (F_{rep} + F_{att})/2 = (F_{rep} - |F_{att}|)/2$.

In Fig. 4(a) a comparison between the free energy of the two cases is presented for strongly charged patches, $\sigma = \pm\eta = 10\kappa_D$. At separations larger than $\kappa_D d > 0.043$, the attractive interaction (oppositely charged surfaces, $\sigma = -\eta$, dashed line) is stronger than the repulsive one (equally charged surfaces, $\sigma = \eta$, solid line). This effect is related to different scaling of the ionic entropy as a function of d for the repulsive

and attractive cases. At smaller separations, $\kappa_D d < 0.043$, the repulsive interaction becomes stronger than the attractive one, and even diverges. The inset shows the overall intersurface interaction as calculated in the simplified nonlinear and linear PB models. It is clear that for large values of σ and η the linear approximation fails to predict the crossover between attraction to repulsion of the nonlinear PB equation.

The origin of the difference between the linear and nonliner PB models stems from the different dependence of the counterions entropy on the intersurface separation d in the case of attraction and repulsion [6,41]. While the entropy in the repulsive case is determined by counter-ion confinement [5], the entropy in the attractive case is governed by counter-ion release [41]. By directly comparing the linear and nonlinear PB solution for strongly and equally charged surfaces, it is found that the counter-ion entropy is largely overestimated in the linear PB solution [42]. This is due to a slower decay of the ionic profile close to charged surfaces in the linear case.

For complementarity, in Fig. 4(b), we present the intersurface interaction of weakly charged surfaces $\sigma = \pm\eta = 0.5\kappa_D$. As expected, the linear approximation agrees well with the simplified nonlinear PB, and the overall interaction is repulsive. These rough estimates suggest a possible crossover as a function of patch charge strength from repulsive to attractive intersurface interaction, but requires further investigations of the nonlinear PB equations for surfaces with finite-size charge patches.

[1] J. N. Israelachvili, *Intermolecular and Surface Forces*, 2nd ed. (Academic Press, New York, 1992).

[2] S. A. Safran, *Statistical Thermodynamics of Surfaces, Interfaces and Membranes* (Westview Press, Boulder, 2003).

[3] D. F. Evans and H. Wennerström, *The Colloidal Domain* (VCH, New York, 1994).

[4] E. J. W. Verwey and J. Th. G. Overbeek, *Theory of the Stability of Lyophobic Colloids* (Elsevier, New York, 1948).

[5] D. Andelman, in *Handbook of Physics of Biological Systems*, edited by R. Lipowsky and E. Sackmann, Vol. I (Elsevier Science, Amsterdam, 1995), Chap. 12.

[6] D. Ben-Yaakov, Y. Burak, D. Andelman, and S. A. Safran, Europhys. Lett. **79**, 48002 (2007).

[7] H. K. Christenson and P. M. Claesson, Adv. Colloid Interface Sci. **91**, 391 (2001).

[8] S. Perkin, N. Kampf, and J. Klein, J. Phys. Chem. B **109**, 3832 (2005).

[9] E. E. Meyer, Q. Lin, T. Hassenkam, E. Oroudjev, and J. N. Israelachvili, Proc. Natl. Acad. Sci. USA **102**, 6839 (2005).

[10] J. Zhang, R. H. Yoon, M. Mao, and W. A. Ducker, Langmuir **21**, 5831 (2005).

[11] S. Perkin, N. Kampf, and J. Klein, Phys. Rev. Lett. **96**, 038301 (2006).

[12] E. E. Meyer, K. J. Rosenberg, and J. N. Israelachvili, Proc. Natl. Acad. Sci. USA **103**, 15739 (2006).

[13] P. Ball, Chem. Rev. **108**, 74 (2008).

[14] M. U. Hammer, T. H. Anderson, A. Chaimovich, M. S. Shell, and J. N. Israelachvili, Faraday Discuss. **146**, 299 (2010).

[15] G. Silbert, D. Ben-Yaakov, Y. Dror, S. Perkin, N. Kampf, and J. Klein, Phys. Rev. Lett. **109**, 168305 (2012).

[16] J. Drelich and Y. U. Wang, Adv. Colloid Interface Sci. **165**, 91 (2011).

[17] I. Popa, G. Gillies, G. Papastavrou, and M. Borkovec, J. Phys. Chem. B **114**, 3170 (2010).

[18] P. Richmond, J. Chem. Soc., Faraday Trans. II **70**, 1067 (1974).

[19] P. Richmond, J. Chem. Soc., Faraday Trans. II **71**, 1154 (1975).

[20] V. M. Muller and B. V. Derjaguin, Colloids Surface **6**, 205 (1983).

[21] M. Kostoglou and A. J. Karabelas, J. Colloid Interface Sci. **151**, 534 (1992).

[22] S. J. Miklavic, D. Y. C. Chan, L. R. White, and T. W. Healy, J. Phys. Chem. **98**, 9022 (1994).

[23] W. J. C. Holt and D. Y. C. Chan, Langmuir **13**, 1577 (1997).

[24] A. V. M. Khachatourian and A. O. Wistrom, J. Phys. Chem. B **102**, 2483 (1998).

[25] J. Stankovitch and S. L. Carnie, J. Colloid Interface Sci. **216**, 329 (1999).

[26] D. Velegol and P. Thwar, Langmuir **17**, 7687 (2001).

[27] S. J. Miklavcic, J. Chem. Phys. **103**, 4794 (1995).

[28] T. O. White and J. P. Hansen, J. Phys.: Condens. Matter **14**, 7649 (2002).

[29] D. B. Lukatsky, S. A. Safran, A. W. C. Lau, and P. Pincus, Europhys. Lett. **58**, 785 (2002).

[30] D. B. Lukatsky and S. A. Safran, Europhys. Lett. **60**, 629 (2002).

[31] C. C. Fleck and R. R. Netz, Europhys. Lett. **70**, 341 (2005); Eur. Phys. J. E **22**, 261 (2007).

[32] J. Landy, Phys. Rev. E **81**, 011401 (2010).

[33] A. Naydenov, P. A. Pincus, and S. A. Safran, Langmuir **23**, 12016 (2007).

[34] R. Brewster, P. A. Pincus, and S. A. Safran, Phys. Rev. Lett. **101**, 128101 (2008).

[35] Y. S. Jho, R. Brewster, S. A. Safran, and P. A. Pincus, Langmuir **27**, 4439 (2011).

[36] Y. S. Velichko and M. O. de la Cruz, J. Chem. Phys. **124**, 214705 (2006).

[37] A. Naji and R. Podgornik, Phys. Rev. E **72**, 041402 (2005).

[38] R. Podgornik and A. Naji, Europhys. Lett. **74**, 712 (2006); Y. S. Mamasakhlisov, A. Naji, and R. Podgornik, J. Stat. Phys. **133**, 659 (2008).

[39] See for example: E. Haleva, N. Ben-Tal, and H. Diamant, Biophys. J. **86**, 2165 (2004); J. L. Harden, C. Marques, J.-F. Joanny, and D. Andelman, Langmuir **8**, 1170 (1992); M. Kiometzis and H. Kleinert, Phys. Lett. A **140**, 520 (1989).

[40] V. A. Parsegian and D. Gingell, Biophys. J. **12**, 1192 (1972).

[41] S. A. Safran, Europhys. Lett. **69**, 826 (2005).

[42] See Fig. 1(a) in D. Ben-Yaakov and D. Andelman, Physica A **389**, 2956 (2010).